Spectral properties of rotating electrons in quantum dots and their relation to quantum Hall liquids

Spectral properties of rotating electrons in quantum dots and their relation to quantum Hall liquids

M Koskinen[1]**, S M Reimann**[2]**, J-P Nikkarila**[1] **and M Manninen**[1]

[1] NanoScience Center, Department of Physics, University of Jyväskylä, FIN-40014, Finland
[2] Mathematical Physics, Lund Institute of Technology, SE-22100 Lund, Sweden

Abstract

The exact diagonalization technique is used to study many-particle properties of interacting electrons with spin, confined in a two-dimensional harmonic potential. The single-particle basis is limited to the lowest Landau level. The results are analysed as a function of the total angular momentum of the system. Only at angular momenta corresponding to the filling factors 1, 1/3, 1/5, etc is the system fully polarized. The lowest energy states exhibit spin waves, domains, and localization, depending on the angular momentum. Vortices exist only at excited polarized states. The high angular momentum limit shows localization of electrons and separation of the charge and spin excitations.

(Some figures in this article are in colour only in the electronic version)

1. Introduction

Semiconductor quantum dots have been a rich playground for both experimental and theoretical physics [1, 2]. Nearly all methods of many-particle physics have been used to study the ground-state properties and excitations in this well-defined problem of a few electrons trapped in a two-dimensional harmonic potential. The research has revealed the existence of a shell structure, Hund's first rule and many other properties related to atomic physics.

In the presence of strong external magnetic fields the quantum dot is a finite-size realization of the quantum Hall liquid (QHL). In fact, it is one of the three geometries (sometimes called the disc geometry) for performing exact many-particle calculations for QHLs. The other two geometries are the surface of a sphere, and a torus [5–7]. In a strong magnetic field, the electron system becomes polarized. Beyond magnetic field strengths corresponding to filling factor $\nu = 1$ in a QHL (or equivalently, to the maximum density droplet in a circular quantum dot) the spin does not usually play a role. Nevertheless, several interesting phenomena, like edge reconstruction [3, 4] and the formation of vortices [8, 9, 11, 12, 10], as well as magnetic excitations [13, 14], have been observed.

The Zeeman effect can be effectively diminished by choosing the material parameters such that the effective Landé factor is zero [15]. In so-called bilayer QHLs, a pseudo-spin

gives the spin-like internal degree of freedom (without the Zeeman effect). The spin degree of freedom drastically changes the 'simple' excitations of the QHL. The integer and the fractional quantum Hall systems at $\nu = 1/3$, $1/5$, etc stay polarized [16] in their ground state and are thus called ferromagnetic, while at other fractions, like $\nu = 2/3$ and $2/5$, the ground state is a spin singlet ($S = 0$). The QHL with spins has been analysed with numerous theoretical methods [17–24, 5, 25–27]. Many of these studies are aimed at infinite QHLs, using periodic boundary conditions and (necessarily) restricting the numerical diagonalization of the full many-body Hamiltonian to a few particles.

The purpose of this paper is to study systematically the properties of many-particle spectra of simple systems in which a small number of electrons are confined in a two-dimensional harmonic potential. We solve the many-particle problem using the configuration interaction (CI) technique, the only approximation being that the single-particle basis is restricted to the lowest Landau level. Since we are mainly interested in large values of the total angular momentum (corresponding to small filling factors) this approximation is suitable. The results show that many features of the spectrum are insensitive to the number of particles in the system and also to the specific form of the inter-electron interaction (remember that the Laughlin Ansatz [28] for the fractional Hall effect does not contain any information about the Coulomb interaction).

In section 2, we will first describe the theoretical methods used. In section 3 we discuss the results for the ground states and low-energy excitations.

2. Theoretical methods

We assume a generic model of interacting electrons in a two-dimensional harmonic potential. The Hamiltonian is

$$H = -\frac{\hbar^2}{2m} \sum_i^N \nabla_i^2 + \sum_i^N \frac{1}{2} m\omega_0^2 r_i^2 + \sum_{i<j}^N \frac{e^2}{4\pi\epsilon_0 |\mathbf{r}_i - \mathbf{r}_j|} \tag{1}$$

where N is the number of particles, m the electron mass, $\mathbf{r} = (x, y)$ a two-dimensional position vector, and ω_0 the oscillation frequency of the confining potential. Alternatively, we can express x and y in polar coordinates, ($x = \text{Re}[r \exp(i\phi)]$, $y = \text{Im}[r \exp(i\phi)]$) or use complex coordinates $z = x + iy$. Note that we do not explicitly consider an external magnetic field. Instead, we solve the many-particle problem for a fixed angular momentum. In the case of a vanishing Zeeman splitting, the only effect of the magnetic field is to increase the orbital angular momentum of the system. The effect of the perpendicular magnetic field (B) would be to add two terms to the Hamiltonian, $\sum m\omega_c^2 r_i^2/8 + \mu_B LB$, where $\omega_c = eB/m$ is the cyclotron frequency, μ_B the Bohr magneton and L the total angular momentum. The ω_c-term would only make the change $\omega_0^2 \rightarrow \omega_0^2 + \omega_c^2/4$ while the second term would only make an L-dependent shift to the total energies. The angular momenta we consider could be reached in usual semiconductor quantum dots with external magnetic fields of $5 \cdots 20$ T [2].

In addition to the Coulomb interaction, we also consider a contact interaction, $V_0 \delta(\mathbf{r}_i - \mathbf{r}_j)$, between the electrons. Note that, trivially, in this case only electrons with opposite spins interact. The Pauli exclusion principle forbids two electrons with the same spin being at the same point.

The Hamiltonian equation (1) is solved by using the configuration interaction (CI) method, with the single-electron basis consisting of harmonic oscillator states in the lowest Landau level (LLL)

$$\psi_\ell(r, \phi) = A_\ell r^\ell e^{-m\omega_0 r^2/2\hbar} e^{i\ell\phi}, \tag{2}$$

where A_ℓ is a normalization factor and ℓ the single-particle angular momentum. In this basis, the diagonal part of the many-particle Hamiltonian is constant, $(L + N)\hbar\omega_0$, L being the total angular momentum. It is then sufficient to diagonalize the interaction part only. Therefore, the role of the strength of the confining potential, ω_0, is only to set the energy scale. In the LLL the structures of the many-particle spectrum and the many-particle wavefunction are completely independent of both ω_0 and the strength of the electron–electron interaction $(e^2/4\pi\epsilon_0)$. The restriction of the single-particle space to the LLL yields the exact result only in the weak interaction limit. However, independently of the strength of the interaction, this approximation becomes more and more accurate when the total angular momentum of the system increases [29]. For the numerical calculation of Coulomb matrix elements, see Stone *et al* [30].

We diagonalize the Hamiltonian matrix for a fixed total angular momentum L and a fixed z-component of the total spin, S_z. We do not fix the total spin, but resolve its value from the eigenstates by taking the expectation value of the $\hat{S}^2$ operator. By selecting $S_z = 0$ for an even number of electrons ($S_z = 1/2$ for an odd number) the diagonalization of the Hamiltonian gives the energies and eigenstates for all possible values of the total spin. The dimension of the Fock space increases quickly with N and L. For example, for $N = 4$, $L = 30$ the matrix dimension is 1234, but for $N = 7$, $L = 42$ it is already 43 600. For large systems ($N > 4$) we make a further reduction of the Fock space by restricting the maximum single-particle angular momentum of the space to be ℓ_{max}. The values used for ℓ_{max} are given in the figure and table captions. In each case ℓ_{max} was chosen to be so large that increasing it does not change the results within the accuracy shown. (For example, in the case of $N = 8$, $L = 56$ we give results with $\ell_{max} = 19$ (figure 12). The use of $\ell_{max} = 17$ would change the ground-state interaction energy by 0.001% and the excitation energies for the lowest five excitations by less than 1%.) The numerical diagonalization was made using the Lanczos method [31]. It gives us the ground state and low-lying excited states.

The symmetry of the system requires that the total electron densities and spin densities are circularly symmetric for all the states. In order to study the internal structure, we thus have to determine the correlation functions. Here we use spin-dependent pair-correlation functions

$$g_{\uparrow\sigma}(\mathbf{r}, \mathbf{r}') = \langle\Psi|\hat{n}_\uparrow(\mathbf{r})\hat{n}_\sigma(\mathbf{r}')|\Psi\rangle, \tag{3}$$

where $|\Psi\rangle$ is the many-particle state in question, σ denotes spin up ($\uparrow$) or down ($\downarrow$), and $\hat{n}_\uparrow$ is the spin-up density operator. We define the total pair-correlation as

$$g(\mathbf{r}, \mathbf{r}') = \tfrac{1}{2}(g_{\uparrow\uparrow}(\mathbf{r}, \mathbf{r}') + g_{\uparrow\downarrow}(\mathbf{r}, \mathbf{r}')). \tag{4}$$

The total angular momentum L can be related to the filling factor ν via the relation

$$\nu \approx \frac{N(N-1)}{2L}. \tag{5}$$

For small particle numbers, this relation is strictly valid only for filling factors $\nu = 1, 1/3, 1/5, \ldots$, i.e. for those states of the fractional quantum Hall effect which can be approximately described by the Laughlin wavefunction [28].

Within the LLL, the smallest possible angular momentum is $L_2 = N(N/2 - 1)/2$, corresponding to a single Slater determinant where the spin-up and spin-down states are occupied from $\ell = 0$ to $N/2 - 1$ (for an even number of particles). It is natural to associate this state to filling factor $\nu = 2$, while equation (5) would give $\nu \approx 2(1 + 1/N)$. Similarly, for fractional filling factors 2/3 and 2/5, etc, equation (5) gives only an estimate of the corresponding angular momentum.

We call the state with filling factor one the maximum density droplet (MDD) [33]. In this case, the angular momentum is well defined, $L_{MDD} = N(N - 1)/2$.

At large angular momenta the electrons crystallize in a rotating Wigner molecule [32, 34–36]. In this case the *charge excitations* can be described by classical vibrations of the molecule, separated from the *spin excitations* of the system. The equilibrium positions of classical electrons depend on the angular velocity ω_r or angular momentum $L = I\omega_r$ of the Wigner molecule (I is the moment of inertia $I = \sum mr_i^2$), and they can be solved by minimizing the classical energy

$$E_{cl}^0(L) = \frac{1}{2}m\omega_0^2\sum_i^N r_i^2 + \sum_{i<j}\frac{e^2}{4\pi\epsilon_0|\mathbf{r}_i - \mathbf{r}_j|} + \frac{L^2}{2m\sum r_i^2}. \tag{6}$$

The eigenfrequencies of the vibrations can then be solved from the equations of motion of the rotating frame (by linearizing the equations around the equilibrium positions of electrons) [36]. Quantization of the rotational and vibrational modes gives an estimate for the energy spectrum

$$E_{QM} = E_{cl}^0 + \sum_k \hbar\omega_k(n_k + \tfrac{1}{2}) + \hbar\omega_0(n_0 + 1), \tag{7}$$

where ω_k are all the vibrational frequencies determined in the rotating frame and $n_k = 0, 1, 2, \ldots$, and the last term corresponds to the centre-of-mass excitations.

Once localized, the electrons form a system where the charge and spin excitations begin to separate. This is most clearly seen in one-dimensional systems [37]. In the case of quasi-one-dimensional quantum rings the whole many-particle spectrum can be quantitatively described with a model Hamiltonian [38, 39]

$$H_{model} = \frac{\hbar^2 L^2}{2I} + \sum_\alpha \hbar\omega_\alpha\left(n_\alpha + \frac{1}{2}\right) + J\sum_{i,j}\hat{S}_i \cdot \hat{S}_j, \tag{8}$$

which consists of rigid rotations, vibrational modes of the localized electrons and of the Heisenberg model for the spin configuration.

3. Results

3.1. Oscillating towards ferromagnetism, $2 \geqslant \nu \geqslant 1$

Figure 1 shows the total spin for the system of $N = 6$ and 10 electrons as a function of the angular momentum. The spin increases, oscillating between zero and its maximum values, up to $S = N/2$, which is the spin of the maximum density droplet (MDD). Note that at this point the electron system is fully polarized (i.e., ferromagnetic). The lowest possible angular momentum for $N = 10$ (in the LLL) is $L = 20$. The corresponding state can be written as

$$\Psi_{\nu=2} = \prod_{i<j}^{N/2}(z_i - z_j)\prod_{k<l}^{N/2}(\tilde{z}_k - \tilde{z}_l)e^{-\sum|z|^2} \tag{9}$$

where we denote the coordinates with the spin-down electrons as $\tilde{z}$. In the occupation number representation we write this 'double MDD' as

$$|\Psi_{(L=20)}\rangle = \left|\begin{array}{ccccccccccccc} \uparrow & \uparrow & \uparrow & \uparrow & \uparrow & 0 & 0 & 0 & 0 & 0 & 0 & 0 & 0 & 0 \\ \downarrow & \downarrow & \downarrow & \downarrow & \downarrow & 0 & 0 & 0 & 0 & 0 & 0 & 0 & 0 & 0 \end{array}\right\rangle,$$

where the arrows show the occupied states of the LLL with increasing order of the single-particle angular momentum. The wavefunction of the MDD, with $S_z = N/2$, is exactly the Laughlin state

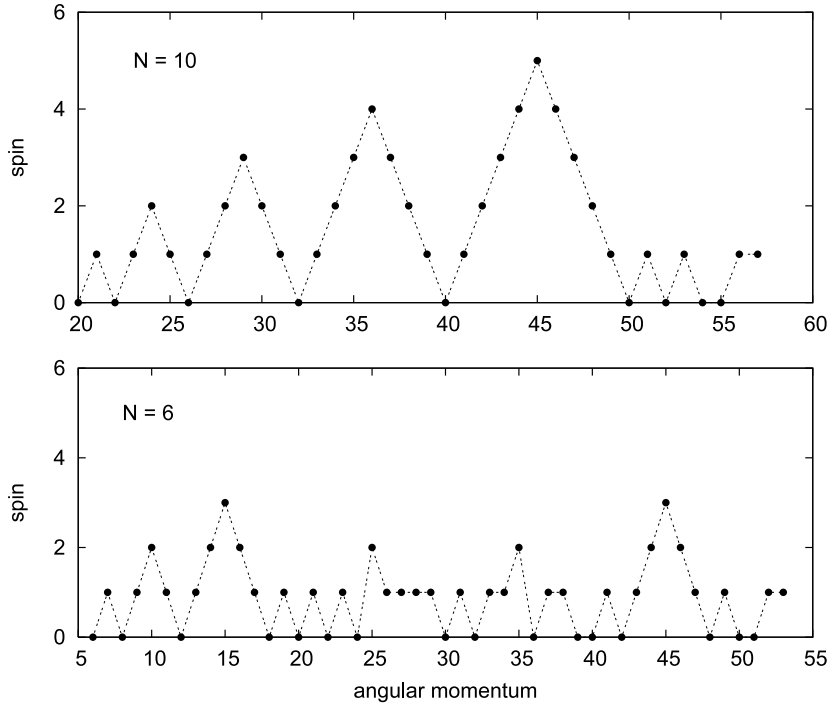$$\Psi_{MDD} = \prod_{i,j}(z_i - z_j)e^{-\sum|z|^2}, \tag{10}$$

Figure 1. Total spin of the lowest energy state as a function of the angular momentum for $N = 10$ and 6 particles ($\ell_{\text{max}} = 29$).

which in the occupation number representation is

$$|\Psi_{\text{MDD}}\rangle = \begin{vmatrix} \uparrow & \uparrow & \uparrow & \uparrow & \uparrow & \uparrow & \uparrow & \uparrow & \uparrow & \uparrow & 0 & 0 & 0 & 0 \\ 0 & 0 & 0 & 0 & 0 & 0 & 0 & 0 & 0 & 0 & 0 & 0 & 0 & 0 \end{vmatrix}.$$

The MDD has a spin degeneracy $2S + 1$. For a given S_z the state can be written as

$$\Psi_{\text{MDD}} = \prod_{i<j}^{N/2+S_z} (z_i - z_j) \prod_{k<l}^{N/2-S_z} (\tilde{z}_k - \tilde{z}_l) \prod_{m,n} (z_m - \tilde{z}_n) \mathrm{e}^{-\sum |z|^2}. \tag{11}$$

It is important to note that for $S_z < N/2$ the above wavefunction is a linear combination of several Slater determinants. For example, for $S_z = 0$, these determinants are of the type

$$\begin{vmatrix} \uparrow & 0 & 0 & \uparrow & 0 & \uparrow & \uparrow & \uparrow & 0 & 0 & 0 & 0 & 0 & 0 \\ 0 & \downarrow & \downarrow & 0 & \downarrow & 0 & 0 & 0 & \downarrow & \downarrow & 0 & 0 & 0 & 0 \end{vmatrix},$$

i.e. there is one electron at each angular momentum from 0 to $N - 1$, but its spin can be up ($\uparrow$) or down ($\downarrow$). It is interesting to note that in the LLL approximation the exact wavefunction of the MDD is the (ferromagnetic) Laughlin state, although one would expect that much stronger correlations could be obtained by also allowing configurations with two opposite spins at the same angular momentum.

It is now easy to understand the maxima before the MDD; see figure 1. They consist of two maximum density droplets of different size, for example

$$|\Psi_{(L=24)}\rangle = \begin{vmatrix} \uparrow & \uparrow & \uparrow & \uparrow & \uparrow & \uparrow & \uparrow & 0 & 0 & 0 & 0 & 0 & 0 & 0 \\ \downarrow & \downarrow & \downarrow & 0 & 0 & 0 & 0 & 0 & 0 & 0 & 0 & 0 & 0 & 0 \end{vmatrix}.$$

Table 1. Overlaps of the wavefunctions calculated with Coulomb and contact interaction for ten electrons. L is the angular momentum and S_i the spin of the state. The subscripts 0 and 1 refer to the lowest energy state and the first excited state, respectively. For $L = 44$ and 45 the overlaps marked by $*$ are those between the first excited state for Coulomb, and the second excited state for contact interaction ($\ell_{max} = 29$).

L	S_0	$|\langle\Psi_C|\Psi_\delta\rangle_0|^2$	S_1	$|\langle\Psi_C|\Psi_\delta\rangle_1|^2$
40	0	0.979	1	0.979
41	1	0.985	2	0.985
42	2	0.991	3	0.991
43	3	0.996	4	0.997
44	4	0.999	2	0.785*
45	5	1	3	0.977*

These states were also studied in [40]. The states in between the maxima are more complicated and can no longer be described by a single determinant. For example, for $L = 40$, the most important configuration

$$\left|\begin{array}{cccccccccccccc} \uparrow & 0 & \uparrow & 0 & \uparrow & 0 & \uparrow & 0 & \uparrow & 0 & 0 & 0 & 0 & 0 \\ \downarrow & 0 & \downarrow & 0 & \downarrow & 0 & \downarrow & 0 & \downarrow & 0 & 0 & 0 & 0 & 0 \end{array}\right\rangle$$

has only 1.5% weight in the exact wavefunction.

Figure 1 shows that at small angular momenta (large filling factor) the system has a tendency to ferromagnetism. The states between the MDDs can be understood as spin waves (or spin excitations) of the ferromagnetic system, as explained in the following section. The oscillations with increasing angular momentum, until the ferromagnetic MDD is reached, see figure 1, are independent of the particle number.

The results for the LLL in the region $2 \geqslant \nu \geqslant 1$ are 'universal', i.e. *independent of the electron–electron interaction*. We repeated the calculations with a contact interaction. The resulting dependence of the total spin on the angular momentum was found to be the same as for the Coulomb interaction. Moreover, the simple states for the spin maxima are identical, and those in between are also very similar. Table 1 shows overlaps of the many-particle states ($|\langle\Psi_{Coulomb}|\Psi_{delta}\rangle|^2$) for different angular momenta. The results demonstrate that for each angular momentum the lowest energy state is the same, but the order of the excited states can depend on the range of the interaction.

For the MDD the overlap equals one, since in both cases the state is the simple Laughlin state of equation (11) (consisting for $N = 10$ electrons of 256 Slater determinants with the same weight). To appreciate the good overlap between the more complicated states, one should note that, for example, for $L = 40$ the 1000 most important Slater determinants only contribute 97.0% of the total wavefunction.

3.2. Spin excitations of the ferromagnetic state

The completely polarized MDD is the ferromagnetic integer quantum Hall state [41, 42, 16]. When the angular momentum is increased, the polarization decreases linearly to zero at angular momentum $L = L_{MDD} + N/2$. At larger angular momenta, the total spin of the lowest energy state is small, usually 0 or 1, until one approaches the filling factor $\nu = 1/3$, where the system again becomes polarized, as seen in figure 1 for six electrons ($\nu = 1$ corresponds to $L = 15$ and $\nu = 1/3$ to $L = 45$).

Figure 2 shows the oscillations in the total energy for ten electrons as a function of the angular momentum. The curves are obtained by subtracting a third-order polynomial fit from
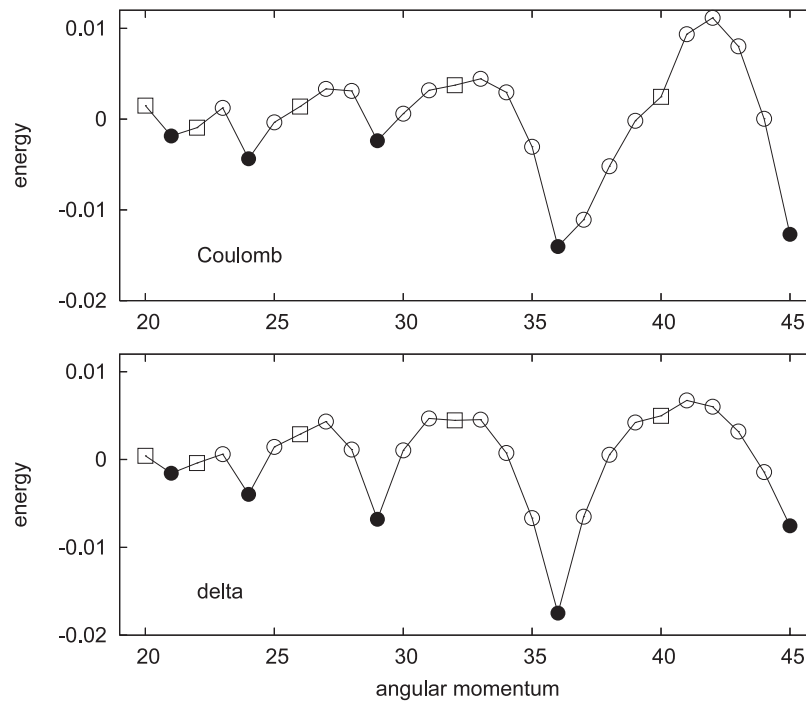
Figure 2. Total energy as a function of the angular momentum for ten electrons interacting with Coulomb interaction (upper panel) or delta function interaction (lower panel). Black dots indicate the states with local spin maxima (see figure 1) and the squares the $S = 0$ states. The energy is obtained by subtracting a third-order polynomial fit from the total energy ($\ell_{max} = 29$).

the total energy. The oscillating part of the total energy, here in the interval $L = 20$–45, is similar for Coulomb and contact interactions. The downwards cusps correspond to the spin maxima. As explained above, these states consist of two maximum density droplets with different size for spin-up and spin-down electrons.

To understand the nature of the other states, we first study the excitation spectrum at the vicinity of the MDD. Figure 3 shows the energy spectrum for ten particles from $L = 40$ to 50. To illustrate the symmetry of the spectrum around the MDD ($L = 45$), we subtract a linear function from the total energy. Figure 3 shows $\Delta E = E - \hbar\omega_0(L+1) - 19.86 + 0.162L$, where the last two terms are obtained by fitting a linear function of the interaction energy (between $L = 40$ and 50). The spectrum is shown for the Coulomb interaction. In the case of the contact interaction, the energy differences between the different spin states disappear after the MDD. The reason is that the MDD wavefunction, equation (10), has zero amplitude whenever two electrons are at the same position and, consequently, the interaction energy of the contact interaction is zero. Beyond the MDD, the wavefunction can be constructed by multiplying the MDD state with a symmetric homogeneous polynomial [43].

Figure 3 has a remarkable similarity with results in the study by Wójs and Quinn [25, 6], who considered a small number of electrons on the surface of a sphere. A similar spectrum is also obtained when using the geometry of a torus [7]. The structure of the spectrum seems then to be independent of the boundary conditions, though in each case the meaning of the angular momentum is different.

The polarized state is the lowest energy state only at the MDD (and at the higher Laughlin states). For other angular momenta, the spin is reduced.
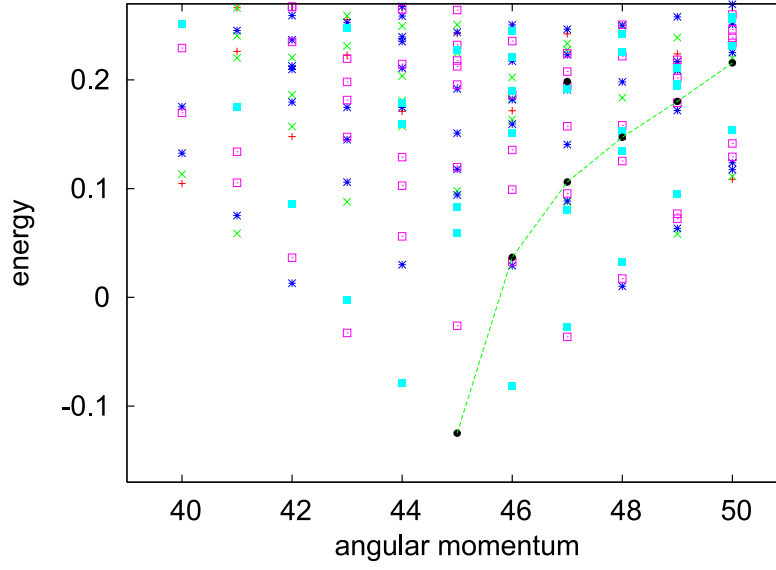
Figure 3. Energy spectrum around the maximum density droplet of ten electrons. Different symbols denote different spin: $S = 5$, black dots; $S = 4$, blue filled squares; $S = 3$, red open squares; $S = 2$, blue stars; $S = 1$, green ×; $S = 0$, red +. The lowest energies for the fully polarized states are connected with a line ($\ell_{max} = 29$).

The spin of the ferromagnetic MDD can be reduced by spin-wave excitations (these are called spin waves [25], spin excitations [19] or exciton superpositions [26]). The operator that excites spin waves can be written as [19]

$$\Sigma_1^+ = \sum_{\ell=0}^{N} \sqrt{\ell + 1} \, c_{\ell+1\downarrow}^+ c_{\ell\uparrow} \tag{12}$$

where c is the normal fermion annihilation operator. Note that operating with Σ_1^+ to the MDD-state, the angular momentum is increased by one and the total spin is decreased by one. Similarly, we can form spin waves which lower the angular momentum:

$$\Sigma_1^- = \sum_{\ell=1}^{N} \sqrt{\ell} \, c_{\ell-1\downarrow}^+ c_{\ell\uparrow}. \tag{13}$$

Moreover, assuming the spin waves as independent excitations, as in the theory of ferromagnetism [44], we can create two or more spin waves by operating successively with the above operators; for example, the state with two spin waves and angular momentum $L = L_{MDD} + 2$ is (without normalization)

$$|\Psi_{2SW}\rangle = \sum_{\ell_1 < \ell_2}^{N} \sqrt{(\ell_1 + 1)(\ell_2 + 1)} c_{\ell_1+1\downarrow}^+ c_{\ell_1\uparrow} c_{\ell_2+1\downarrow}^+ c_{\ell_2\uparrow} |\psi_{MDD}\rangle. \tag{14}$$

Table 2 shows overlaps between the exact result and that of the spin-wave approximation. For the single spin wave the results agree with those of Oaknin *et al* [19]. For $N = 10$ electrons, the overlap decreases with the number of the spin waves, but is still more than 60% for four spin waves. However, for the singlet state, which requires five spin waves, the overlap is less than 30%. Clearly, this singlet state has a different character. This state ($L = 40$ for $N = 10$) also
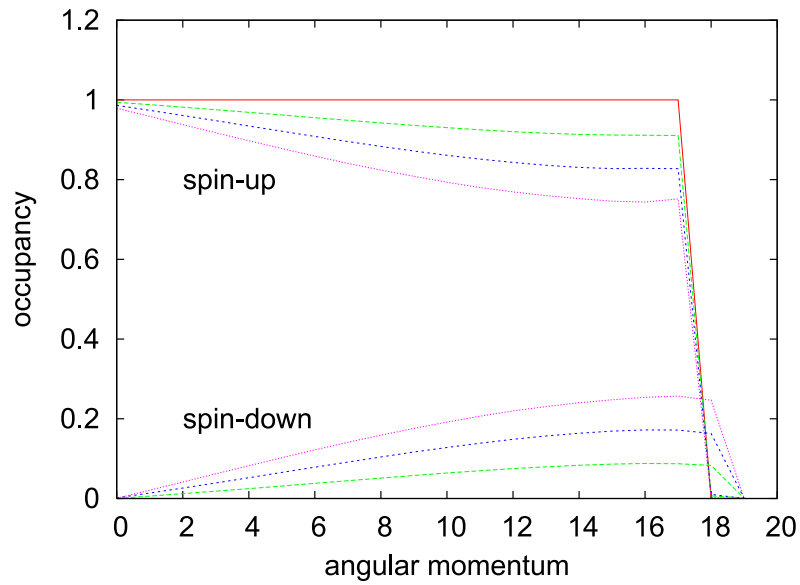
Figure 4. Occupation of the single-particle levels of the lowest state at different angular momenta for 18 electrons. Solid (red) line: $L = 153$ (MDD), long-dashed (green) line: $L = 154$, short-dashed (blue) line: $L = 155$, dotted (pink) line: $L = 156$ ($\ell_{max} = 21$).

Table 2. Overlap between the exact result and the spin-wave states. N, L, and S are the number of electrons, angular momentum and total spin, respectively. n is the number of spin waves ($\ell_{max} = 29$ for $N = 10$, ($\ell_{max} = 21$) for $N = 18$).

N	L	S	n	$|\langle\Psi|\Psi_{nSW}\rangle|^2$
10	40	0	5	0.296
10	41	1	4	0.647
10	42	2	3	0.844
10	43	3	2	0.941
10	44	4	1	0.986
10	45	5	0	1 (MDD)
10	46	4	1	0.972
10	47	3	2	0.913
10	48	2	3	0.803
10	49	1	4	0.607
10	50	0	5	0.262
18	153	9	0	1 (MDD)
18	154	8	1	0.990
18	155	7	2	0.971
18	156	6	3	0.957

shows a small kink in the total energy as a function of the angular momentum (see figure 2). We will return to this state in the next section. Oaknin *et al* [19] have shown that by projecting the simple spin-wave state, equation (12), to a state which is orthogonal to the centre-of-mass excitations, the overlaps become even better.

Table 2 shows that when the number of electrons increases, the approximation of independent spin waves gets more accurate. For $N = 18$ electrons, even the three spin waves describe the exact result with 96% accuracy. Figure 4 shows the single-particle occupancy of
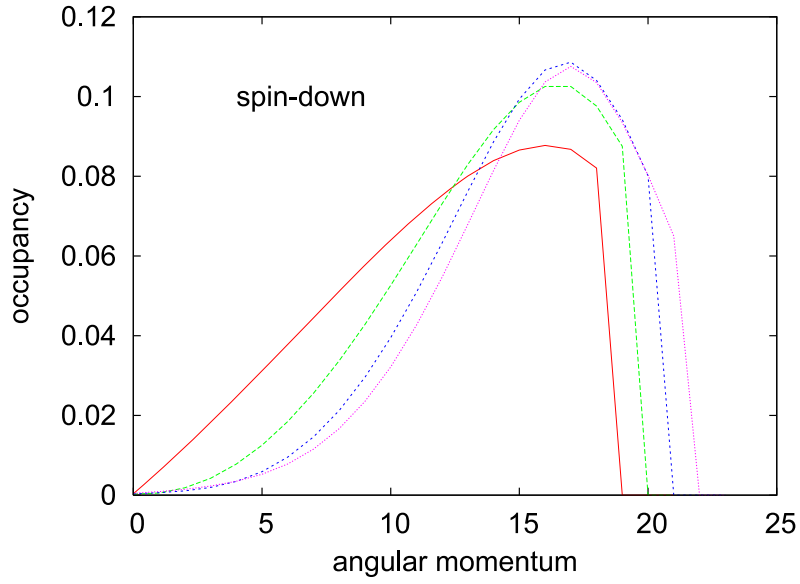
Figure 5. Occupation of the single-particle levels of the lowest $S = 8$ state at different angular momenta for 18 electrons. Solid (red) line: $L = 154$ (MDD), long-dashed (green) line: $L = 155$ short-dashed (blue) line: $L = 156$, dotted (pink) line: $L = 157$. (The solid (red) line is the same as the lower long-dashed (green) line in figure 4. Note the different scale, $\ell_{max} = 21$.)

the exact states corresponding to one, two and three spin waves for 18 electrons. Clearly, the occupancy of the minority spin states (spin down) increases linearly as a function of the single-particle angular momentum (for small angular momenta) in agreement with the spin-wave suggestion, equation (12). Moreover, the increase of the spin waves increases the occupancy linearly. These observations are in qualitative agreement with the theory of Doretto *et al* [27], which shows that the magnetic excitons have bosonic nature.

Increasing the angular momentum from the MDD, the energy spectrum shows a large energy gap between low-energy states and the rest of the states (including the fully polarized state; see figure 3). We demonstrated previously that the lowest of these states consist of spin waves. The highest state below the energy gap has spin $S = N/2 - 1$ in the whole region from $L = L_{MDD} + 1$ up to $L = L_{MDD} + N/2$ (i.e. from $L = 46$ to 50 for $N = 10$). Figure 5 shows that the minority spin concentrates closer and closer to the surface when the angular momentum increases. The total spin density $n_\uparrow - n_\downarrow$ still remains positive at the surface. This suggests that the spins along the surface are slightly tilted [45]. These states are often referred to as having non-collinear (or canted) spins [45, 46]. We should note that in our computations we have chosen S^2 and S_z as good quantum numbers. Consequently, we do not know the values of S_x and S_y.

3.3. Domain walls

Large ferromagnetic systems may form domains. In normal magnetic materials the domains are caused by the long-range dipole interaction and exist already in the ground state. However, even without the dipolar interaction, domains can form as low-energy excitations. This seems to be the case in quantum Hall liquids [21, 16, 24, 47, 48, 5, 49].

In finite small systems, the existence of domains is not as obvious, due to the small number of electrons and the finite thickness of the domain walls. Nevertheless, our results show a clear
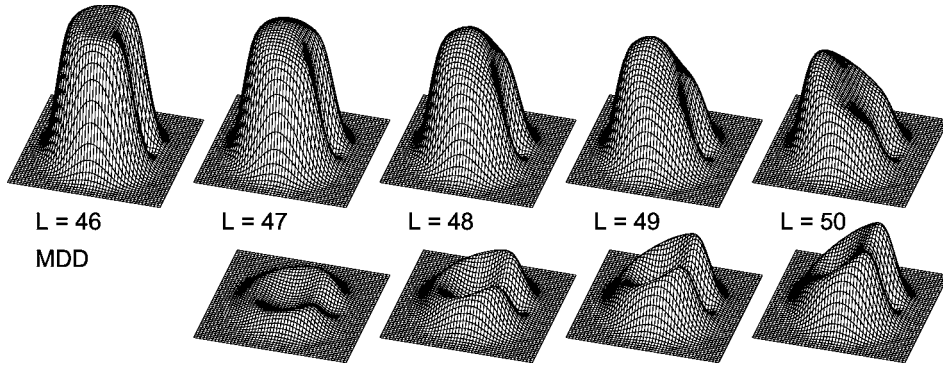
Figure 6. Pair correlation functions beyond the MDD for $N = 10$ electrons. The upper panel shows the up–down correlation $g_{\uparrow\downarrow}$, and the lower panel the up–up correlation, $g_{\uparrow\uparrow}$. The number of spin-down electrons increases from one to five, and the number of spin-up electrons decreases from nine to five when going from left to right ($\ell_{max} = 29$).
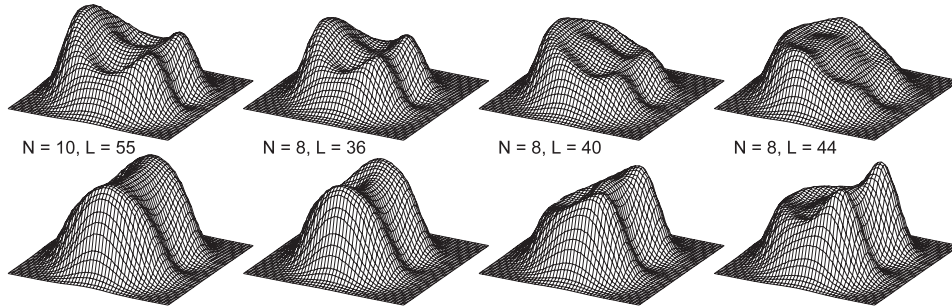

Figure 7. Pair correlations for spin-singlet states after the MDD. The upper row shows the up–down correlation, $g_{\uparrow,\downarrow}$, and the lower row the up–up correlation, $g_{\uparrow,\uparrow}$. The number of electrons N and the angular momentum L are indicated. Note that $N = 10$, $L = 55$ corresponds to the state $N = 8$, $L = 36$ ($\ell_{max} = 29$).

separation of up and down spins at certain angular momenta. Figures 6 and 7 show a set of pair correlations showing the tendency to separate the spin-up and spin-down electrons. The gradual development to a 'domain wall state' is indicated in figure 6, which shows the correlations for a dot with $N = 10$ electrons from angular momenta L_{MDD} to $L_{MDD} + N/2$. The largest of these angular momenta ($L = 50$) shows clearly that the up and down electrons prefer to be at the opposite sides of the dot. Note that in a quantum mechanical system the domain wall is not fixed at a certain place. In the pair correlation the apparent position of the domain wall depends upon the reference point. For example, if the reference electron, say spin up, was at the centre of the dot, the other spin-up electrons would stay closer to the origin, while the spin-down electrons are pushed further out.

The structure of two domains for $L = L_{MDD} + N/2$ is a general feature and does not depend on the number of electrons. Calculations were performed for $N = 6, 8, 10$, and 12 electrons. In all cases, the development of the pair correlation functions appear to be similar to that shown in figure 6 above.

Increasing the angular momentum further results in more complicated domain structures. For angular momentum $L = L_{MDD} + N$, four domains seem to form, as seen in figure 7 for
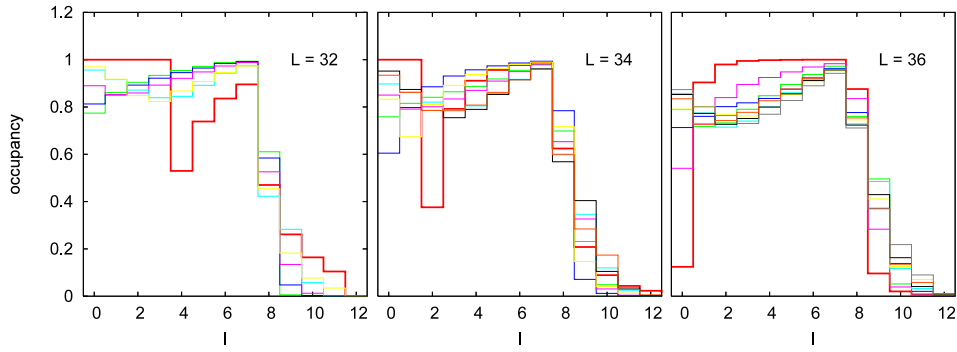
Figure 8. Single-particle occupancy of different energy states for $N = 8$, $L = 32, 34$, and 36. The occupancies of the lowest fully polarized state $S = 4$ are shown by thick red lines, and the states below the first polarized state are shown by thin lines. The polarized results show a clear dip at a given single-particle state as a signature of a single vortex, which reaches the origin at $L = 36$ ($\ell_{max} = 29$).

$N = 8$, $L = 36$ and $N = 10$, $L = 55$. For even larger angular momenta it is not possible to resolve possible domain structures at these small particle numbers. At angular momentum $L = 44$, corresponding to the filling factor $\nu = 2/3$, the pair correlation function cannot be as easily interpreted.

It is important to note that our computations do not contain the dipole–dipole interaction of the magnetic moments of electrons. The origin of the domain formation is thus different from that in normal ferromagnets. An infinite system would not have domains in the ground state. The fact that they appear in the lowest energy state at a fixed angular momentum does not imply that they represent a ground state. The antisymmetry of the total wavefunction restricts the allowed quantum states of a given total angular momentum. For example, the polarized state has lowest energy only for a few angular momenta, while others must have some other internal structure. This becomes clear in the limit of localized electrons, to be discussed later.

3.4. Vortices and edge reconstruction

In a strong magnetic field, the Zeeman effect polarizes the electrons and the system usually stays polarized beyond the maximum density droplet. The low-energy excitations of the MDD are then characterized by vortices [8, 9, 11, 12] or edge reconstruction [33, 4]. As discussed earlier by Yang *et al* [50], when the angular momentum increases from that of the MDD, *holes* will be formed in the otherwise filled Fermi sea below the single-particle angular momentum $\ell = N - 1$. Close to the MDD, the most important configuration of the many-particle state will have only one hole. For example at $L = 32$, $N = 8$ we have

$$\left| \begin{array}{cccccccccccc} \uparrow & \uparrow & \uparrow & \uparrow & 0 & \uparrow & \uparrow & \uparrow & \uparrow & 0 & 0 & 0 \\ 0 & 0 & 0 & 0 & 0 & 0 & 0 & 0 & 0 & 0 & 0 & 0 \end{array} \right\rangle .$$

Increasing the angular momentum, the hole decreases its (single-particle) angular momentum stepwise, 'moving to the left' in the Fock state until it reaches $\ell = 0$. In the full CI calculation for polarized electrons, there are many other possible configurations with the same angular momentum, but this single-hole configuration has the largest weight. This is clearly seen in figure 8, where the thick red line shows the result for polarized electrons ($S = 4$).

The formation of a single hole in the MDD [50] can be understood in two ways. We can consider it as a single-particle excitation, where an electron is excited from $\ell = 4$ to 8.
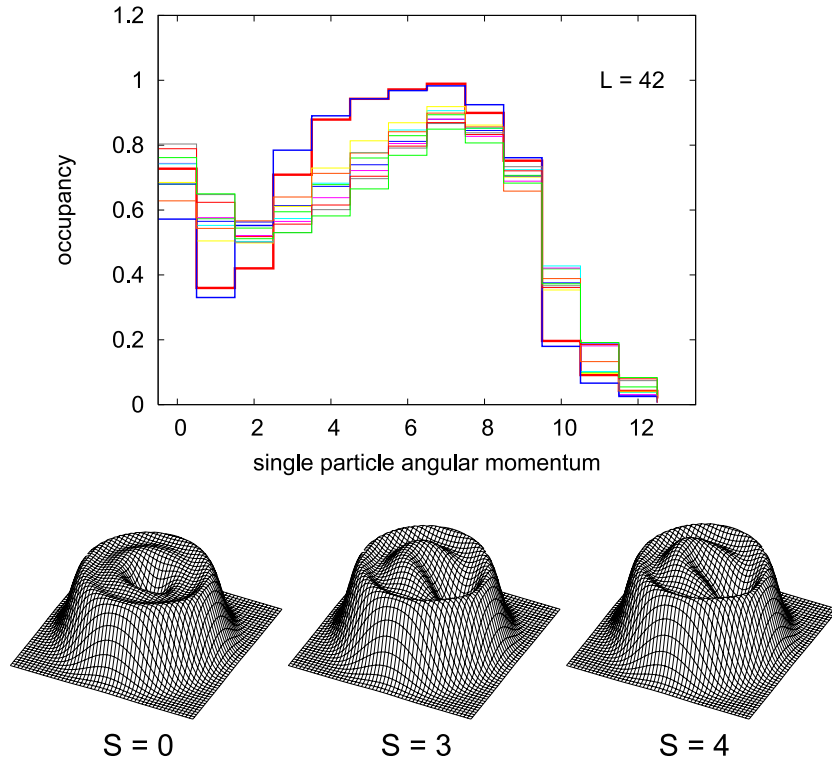
Figure 9. Upper panel: Occupancy of the single-particle angular momenta of the lowest state for $N = 8$, $L = 42$ (thick (red) line), and for the lowest $S = 3$ (thick (blue) line) and $S = 4$ (thick (green) line) states. The lower panel shows the hole–hole correlation functions for the same states ($\ell_{max} = 29$).

Alternatively, we can view it as a collective excitation, where four electrons from $\ell = 4 \cdots 7$ are each excited to the next angular momentum state. The latter interpretation is consistent with the vortex picture in boson systems [9], where the Bose condensate corresponds to the MDD of spinless fermions.

The holes in the electron sea of the MDD can be identified with vortices [51]. The electron density has a minimum at the site of the vortices, the wavefunction phase changes by 2π in going around the vortex centre [9], and the electron current circulates around the vortex [8].

We now return to the case without Zeeman splitting. The total spin of the lowest energy states beyond the MDD is then generally small, and the fully polarized state is a rather high-lying excited state. Figure 8 shows the single-particle occupancies for all the energy states below the polarized states, at angular momenta $L = 32, 34$ and 36. A typical dip in the occupancy at one single-particle angular momentum is seen only in the fully polarized state. The low-spin states show a more uniform reduction of the occupancy and softening of the surface. Vortices seem to be low-energy excitations only for the polarized electron gas.

The most clear two-vortex state in the case of eight electrons is at angular momentum $L = 42$ (for polarized electrons) [9]. In this case, the most important configuration is

$$\left| \begin{array}{cccccccccccc} \uparrow & 0 & 0 & \uparrow & \uparrow & \uparrow & \uparrow & \uparrow & \uparrow & \uparrow & 0 & 0 \\ 0 & 0 & 0 & 0 & 0 & 0 & 0 & 0 & 0 & 0 & 0 & 0 \end{array} \right\rangle.$$

More generally, for n vortices the most important configuration is the one where the n holes are next to each other [51]. Figure 9 shows the single-particle occupancies of the exact

diagonalization for $N = 8$, $L = 42$ for all the states up to the fully polarized state. Again, we see that only in the polarized state, shown by the thick red line, there clearly are two adjacent states ($\ell = 1$ and 2) where the occupancy is small compared to the other states. The only other state which has a rather similar occupancy distribution, is the one with total spin $S = 3$, i.e. the almost fully polarized state, shown by the thick blue line. The other spin states show only a weak minimum at the region of $\ell = 1$ or 2, but larger occupancies from $\ell = 10$ up, i.e. at the surface of the electron cloud. In fact, the general feature of the occupancy distribution for all the states is that there is a maximum at $\ell = 0$ and a broad maximum at larger ℓ, the centre being at about $\ell = 7$. This is the first indication that at high (total) angular momenta the electrons begin to localize. For $N = 8$ electrons, eventually one electron will localize at the centre, while the other seven form a ring around it.

The excited states with $S = 4$ and 3 show occupancy distributions consistent with the existence of two vortices [9]. Other signatures of vortices are the phase of the wavefunction, and the pair correlation functions. The phase is not easy to compute in our formalism. Furthermore, as it is a function of $2N$ coordinates its interpretation is not straightforward [9]. Manninen *et al* [51] have shown that by interpreting the vortices as holes, their localization can be seen clearly in the hole–hole correlation function. Figure 9 shows the hole–hole correlations for the lowest energy state $S = 0$ and for the $S = 3$ and 4 states. The correlations for the high-spin states appear very similar. The reference vortex (or hole) is seen as a deep minimum. At the opposite side, there is a maximum corresponding to the second vortex. The ring around is caused by the holes outside the electron distribution. (In reality, the hole density is constant outside the electron distribution, but since here the available single-particle space is limited, the hole density also goes to zero.) The hole–hole correlation function for the $S = 0$ state does not even show a clear minimum at the site of the reference point (it is filled by the hole with opposite spin). The minimum seen in the case of $S = 0$ is at the centre of the dot and is caused by the fact that the electron density there is large and, consequently, the hole density is small.

For large electron numbers ($N \approx 20$) the vortices of the polarized system can be seen clearly in the many-particle spectrum. The localization of vortices causes periodic oscillations to the spectrum [51] in a similar fashion as the localization of the electrons when their number is small [35]. Unfortunately, we are not yet able to do accurate computations for such large systems, when including the spin degree of freedom. However, the above results for $N = 8$ electrons strongly suggest that while the vortices are low-energy excitations for the polarized electrons, they are not the lowest excitations for electrons with spin.

In the case of polarized electrons, the MDD breaks up by separating a ring of electrons [3, 4]. In the single-particle occupancy, the formation of this so-called Chamon–Wen edge [3] is seen as a minimum in a similar way as the formation of vortices. Indeed, these two phenomena are intimately related. The minimum between the separated electron ring and the rest of the MDD is actually caused by one or two vortices [10, 52]. In the circularly symmetric electron density, the ring of vortices is seen as a minimum. In the vortex–vortex (hole–hole) correlation, however, the vortices are localized along this ring. Again, at present we cannot perform computations for large enough electron numbers to study the possibility of Chamon–Wen edge reconstruction in the low-spin states. However, due its close relation to the vortex formation, we can safely predict that it will only be formed in the excited states with high total spin.

3.5. Spectra between $\nu = 1$ and $\nu = 1/3$

The many-particle low-energy spectrum shows qualitatively similar structures going up or down from the angular momentum $L = N(N-1)$, corresponding to filling factor $\nu = 1/2$. The
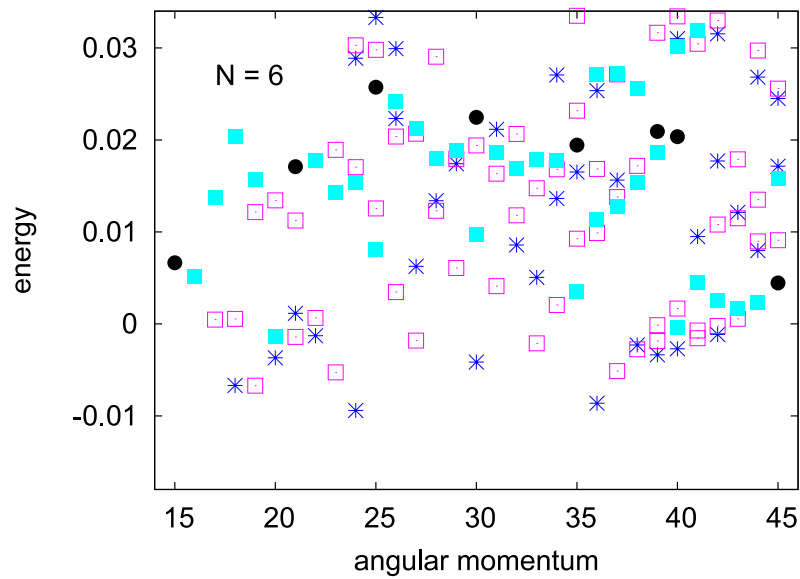
Figure 10. Spectrum for $N = 6$ electrons for filling factors between $\nu = 1$ and $1/3$, as a function of angular momentum. Blue crosses: $S = 0$; blue squares: $S = 1$, red open squares: $S = 2$, black bullets: $S = 3$. A third-order polynomial fitted to the lowest energies has been subtracted from the total energy ($\ell_{max} = 29$).

composite fermion picture of Jain [53, 54] reproduces this 'symmetry' [55] in a very natural way. Subtracting a smooth function of angular momentum, $F(L)$, from the original spectrum removes the downward slope of the interaction energy, so that the small energy differences between the excited states can be more clearly illustrated, and the symmetry around the $\nu = 1/2$ states is mapped out in a very clear way. Figures 10, 11, and 12 show the spectra for six, seven, and eight electrons. In these cases, the function $F(L)$ is a third-order polynomial fitted in each case to the lowest energy states in the interval shown. The filling factor $1/2$ corresponds to angular momenta 30, 42, and 56 for $N = 6$, 7, and 8, respectively. Going up from these angular momenta gives qualitatively the same spectrum as going down, i.e. we have the spin states in the same order and the sizes of the energy gaps are qualitatively similar. At filling factor $1/2$, the lowest state has total spin 0, $1/2$ and 1, for $N = 6$, 7, and 8, respectively. At $L = N(N - 1)/2$ and $L = 3N(N - 1)/2$ ($\nu = 1$ and $\nu = 1/3$) the lowest state is ferromagnetic (has maximum spin). There are two other energetically favourable states, at $L = N(N - 1)/2 + N^2/4$ and $L = 3N(N - 1)/2 - N^2/4$. Our interpretation is that the former of these corresponds to the filling factor $\nu = 2/3$ and the latter to $\nu = 2/5$ (note that equation (5) does not give exactly the above angular momenta for these special filling factors). The structure of the spectra around these special points is independent of the number of electrons (for an odd number of electrons, the lowest spin is naturally $S = 1/2$).

The maximum spin state, $S = N/2$, is the lowest energy state only at angular momenta corresponding to the filling factors $\nu = 1$ (MDD) and $\nu = 1/3$. It is interesting to observe that while the MDD has a large energy gap to the first excited state, the filling factor $\nu = 1/3$ does not. In fact, the energy gaps of the special singlet states at filling factors $\nu = 2/3$ and $2/5$ have much larger energy gaps between the ground state and the lowest excited state. The large excitation gaps at these filling factors are well known; see for example [7].
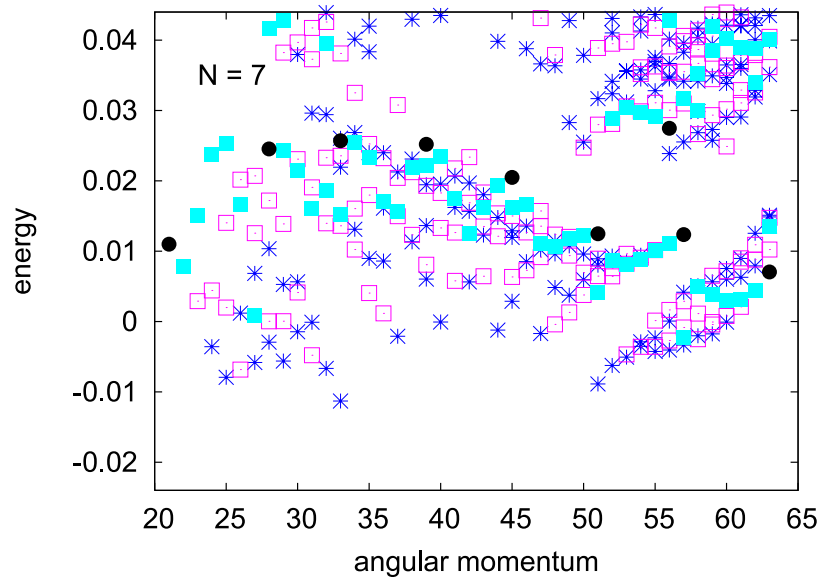
Figure 11. Spectrum for $N = 7$ electrons $\nu = 1 \cdots 1/3$. Blue crosses: $S = 1/2$; blue squares: $S = 3/2$; red open squares: $S = 5/2$; black dots: $S = 7/2$. A third-order polynomial fitted to the lowest energies has been subtracted from the total energy ($\ell_{max} = 19$).
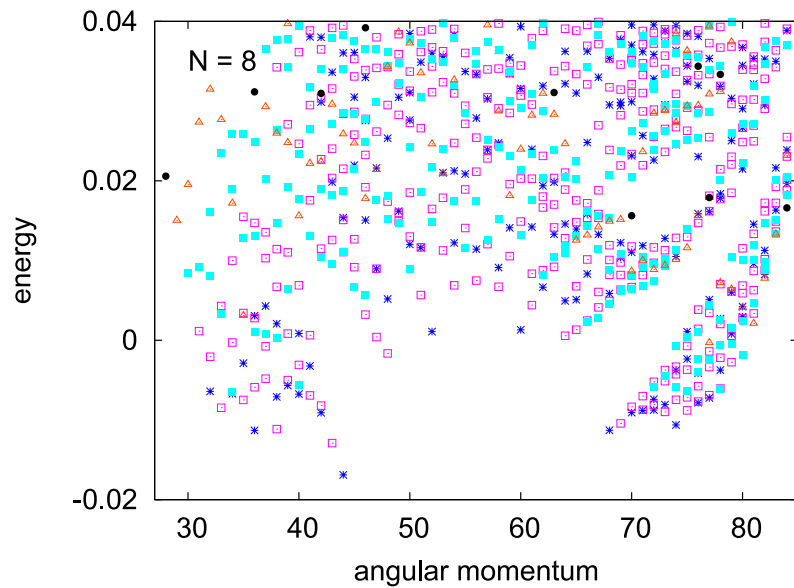

Figure 12. Spectrum for $N = 8$ electrons $\nu = 1 \cdots 1/3$. Blue crosses: $S = 0$; blue squares: $S = 1$; red open squares: $S = 2$; red triangles: $S = 3$; black dots: $S = 4$. A third-order polynomial fitted to the lowest energies has been subtracted from the total energy ($\ell_{max} = 19$).

3.6. Halperin–Haldane wavefunctions

The clear local minimum in the energy at angular momenta $L = N(N-1)/2 + N^2/4$ and $L = 3N(N-1)/2 - N^2/4$ suggests that there is a special way to build correlations

Table 3. Overlap between the exact result and the Halperin–Haldane model, $|\langle\Psi_{HH}|\Psi\rangle|^2$, for different filling factors ν and electron numbers N (for $N = 6$ the cut-off $\ell_{max} = 29$ was used).

N	ν			
	1	$\frac{2}{3}$	$\frac{2}{5}$	$\frac{1}{3}$
2	1	1	1	1
3	1	0.843	0.920	0.982
4	1	0.636	0.931	0.958
5	1	0.363	0.911	0.970
6	1	0.162	0.909	0.794

in the wavefunction. The Ansatz wavefunction for the fractional quantum Hall effect [28], equation (11), can be extended for some of the non-simple fractions as [56, 57]

$$\Psi_{HH} = \prod_{i<j}^{N/2}(z_i - z_j)^q \prod_{k<l}^{N/2}(\tilde{z}_k - \tilde{z}_l)^q \prod_{m,n}^{N/2}(z_m - \tilde{z}_n)^p e^{-\sum|z|^2} \tag{15}$$

where q is an odd integer and p a positive integer which can be even or odd. The angular momenta $L = N(N - 1)/2 + N^2/4$ and $L = 3N(N - 1)/2 - N^2/4$ agree with the above wavefunction with $q = 1$, $p = 2$ and $q = 3$, $p = 2$, respectively. Table 3 shows the calculated overlaps. For the $L = N(N - 1)/2 + N^2/4$ state the overlap decreases rapidly with increasing N. Clearly, the exact quantum state cannot be described by equation (15) for $\nu = 2/3$. In fact, in this case the wavefunction equation (15) is a mixture of the $S = 0$ and 2 states. For $L = 3N(N-1)/2 - N^2/4$ the agreement is much better, indicating that the above wavefunction is a good approximation to the ground state of $\nu = 2/5$. Also, it now has $S = 0$.

It should be noted that for smaller filling factors than $1/3$ (or $1/5$) the above simple analytic Ansatz does not accurately describe the true electron state. In particular, it fails to describe the electron localization. In this region, other trial wavefunctions, like for example the ones suggested by Yannouleas and Landman [58], seem to be a better alternative.

3.7. Symmetry of the spectrum around $\nu = 1/3$

In table 3 above, we showed that after subtracting the smooth part, the resulting energy spectrum is symmetric around the MDD ($\nu = 1$). It is thus interesting to see if similar symmetry exists also around the angular momentum $L = 3N(N - 1)/2$, corresponding to $\nu = 1/3$. Figure 13 shows the excitation spectrum for seven electrons, now plotted such that the centre is around $L = 63$. Again, a smooth function (in this case, a second-order polynomial fitted to the lowest energies in the angular momentum interval shown) is subtracted from the original spectrum. The figure shows that in the immediate vicinity, from $L = 58$ to 68, the spectrum shows a qualitative mirror symmetry for the states in the low-energy band, below the large energy gap. The lower panel of figure 13 shows the order of different spin states for the low-energy band. We can see that, in addition to the symmetry near $L = 63$, there is a repeating period of 6 in the appearance of different spin states in the whole range shown (ignoring their order). This is due to the emergence of the localization of the electrons in a six-fold ring with one electron at the centre, as briefly discussed in the next section.

3.8. Localization of electrons at high angular momentum, $\nu \ll 1/3$

Increasing the angular momentum, the electron cloud in the harmonic confinement expands and the electrons begin to localize. For spinless electrons, it is possible to perform accurate
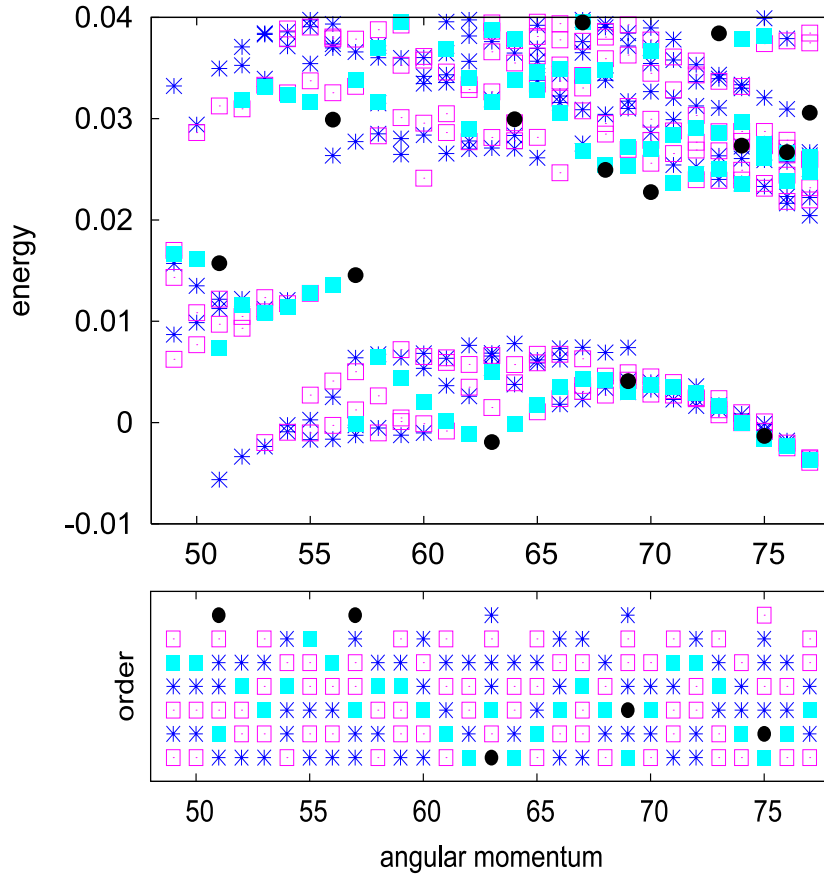
Figure 13. Spectrum for $N = 7$ electrons around angular momentum $L = 63$ ($\nu = 1/3$). Blue crosses: $S = 1/2$; blue squares: $S = 3/2$; red open squares: $S = 5/2$; black bullets: $S = 7/2$. The upper panel shows the energy spectrum with a smooth part subtracted. The lower panel shows the order of different spin states in the low-energy band, below the large energy gap in the spectrum. Note the symmetry around $L = 63$ ($\ell_{max} = 19$).

CI calculations for much higher angular momenta than if spin is included. For small electron numbers, the spectrum shows a characteristic periodicity as a function of the angular momentum [59, 60, 29, 2, 35, 36]. In these studies the number of electrons has been so small that filling factors down to $\nu = 1/9$ have been reached. The results are then consistent with the expectation that in quantum Hall liquids the crystallization is expected [61] to happen at filling factors smaller than $\nu = 1/7$. The periodicity in the spectrum as a function of angular momentum is determined by the symmetry group of the Wigner molecule. Up to five electrons, the localized electrons form a single ring, the period being equal to the number of electrons. From $N = 6$ to 8 electrons, one of the electrons localizes at the centre of the parabolic trap, while the rest form a single ring around it [62, 63]. The length of the period of the oscillations in these cases is then $N - 1$. From figures 11 and 12 we can see clearly that, at high angular momenta, the fully polarized case has a low-energy state only at every fifth and seventh angular momentum, respectively. In the case of six electrons the period of 5 becomes clear only at higher angular momenta than those shown in figure 10 [34, 29], due to the competition of two possible classical configurations of the electrons in the Wigner molecule [62].
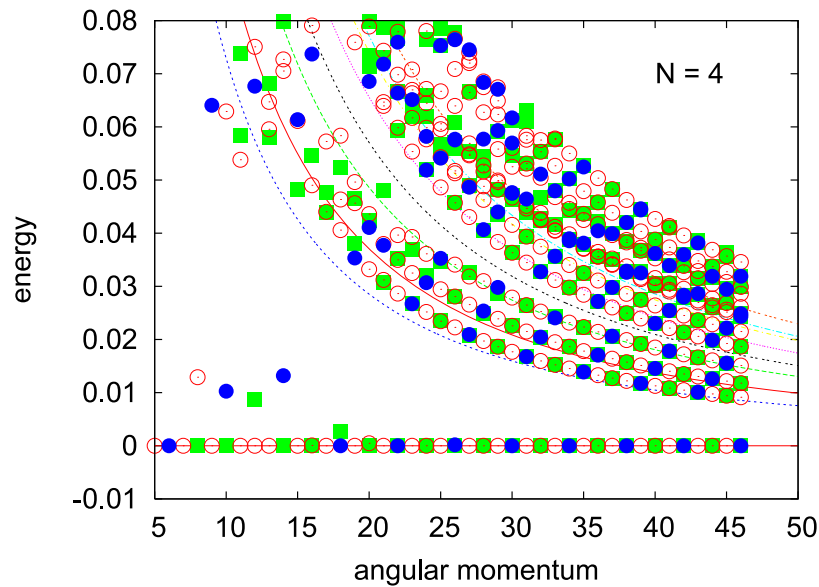
Figure 14. Excitation energies as a function of the angular momentum. Points are results of the exact diagonalization and the lines from the model of classical vibrations. Blue points: $S = 2$, open circles: $S = 1$, green squares: $S = 0$ (no cut-off ℓ_{max} was used).

For polarized (spinless) electrons the tendency for localization is rather insensitive to the interparticle interaction. It appears for long-range Coulomb interactions, as well as for short-range Gaussian interactions. Moreover, similar localization patterns occur for fermions as well as bosons [35]. In all these cases, the effect of the localization is seen as periodic oscillations in the energy as a function of the angular momentum. There is one exception, however. The exactly solvable model of harmonic interparticle interaction does not show this periodicity [64, 43]. The reason is the large degeneracy of the energy states and the fact that, classically, all particles interacting by a repulsive harmonic potential are localized at the origin (otherwise, they would not be confined).

Maksym *et al* [32], and Nikkarila and Manninen [36], using a slightly different approach, have shown that at large angular momenta the whole many-particle spectrum of rotating polarized electrons can be quantitatively described by quantizing the classically determined vibration frequencies of the Wigner molecule. This suggests that the charge excitations (vibrational modes) and the spin excitations will separate in a similar fashion as in one-dimensional quantum rings [38, 39], in which case the system can be described by the Hamiltonian of equation (8).

We determined the vibrational modes of classical electrons in a two-dimensional harmonic confinement using a rotating frame, as in [36], and compared the results with those obtained from the full quantum-mechanical CI calculation.

For $N = 4$ electrons, the result is shown in figure 14. The figure shows the excitation energies for each angular momentum, i.e. the total energy of the excited state minus the lowest energy for the same angular momentum. The quantum-mechanical results approach the classically determined energies when the angular momentum increases. Different spin states of the quantum-mechanical calculation are marked by different symbols. We can see clearly that the lowest energy state and each vibrational state has a periodic pattern of spin states.
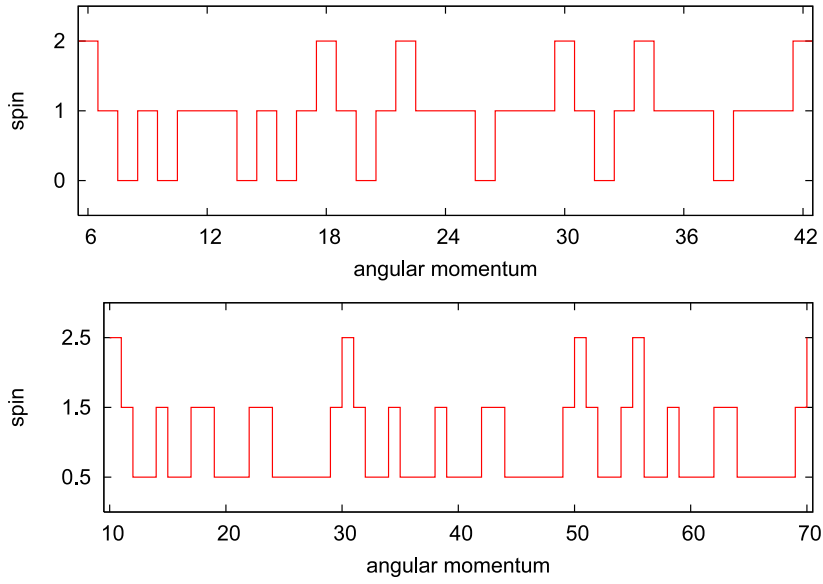
Figure 15. Total spin of the lowest energy state as a function of the total angular momentum for $N = 4$ and 5 ($\ell_{max} = 37$).

The periodic appearance of the different spin states at each vibrational mode in figure 14 gives further support to the separation of the spin and charge excitations. Assuming the model Hamiltonian of equation (8), one can use group theory [65, 38, 66] to analyse which spin state corresponds to which angular momentum. The Heisenberg coupling constant J determines the energy splitting of different spin states, and its sign determines if the electron system is ferromagnetic or anti-ferromagnetic. Indeed, the obtained spin states agree well with the prediction of the model Hamiltonian. However, the simple model cannot explain quantitatively the energy differences between the different spin states. For example, for angular momenta 18, 22, 24, etc, the purely rotational band has spin states $S = 2$ and 0. If the Heisenberg coupling were ferromagnetic, the $S = 2$ state would have lower energy than the $S = 0$ state, while for anti-ferromagnetic coupling, this would be the other way around.

Figure 15 shows the total spin of the lowest energy states for four and five electrons as a function of the angular momentum. Clearly, we can see that neither of these cases show a simple period of N, as would be expected from a simple Heisenberg model of localized electrons.

In the case of one electron per lattice site the Hubbard model approaches the anti-ferromagnetic Heisenberg model [67]. Since here the electrons are localized in a Wigner lattice, one should expect that the same model works equally well (although now the electrons are localized not by external potential, but by the mean field created by the other electrons). For quasi-one-dimensional quantum rings this indeed was shown to be the case [38, 39], as well as for electrons localized in the corners of triangular or square quantum dots [68]. However, the result of figure 15 shows clearly that this does not hold for electrons localized in a two-dimensional harmonic confinement.

We can mimic a quantum ring by restricting the single-particle basis from low and high angular momenta, i.e. $\ell_{min} \leqslant \ell \leqslant \ell_{max}$. Figure 16 shows part of the energy spectrum computed with this restricted basis compared to that of the full calculation. The result for the 'ring' shows
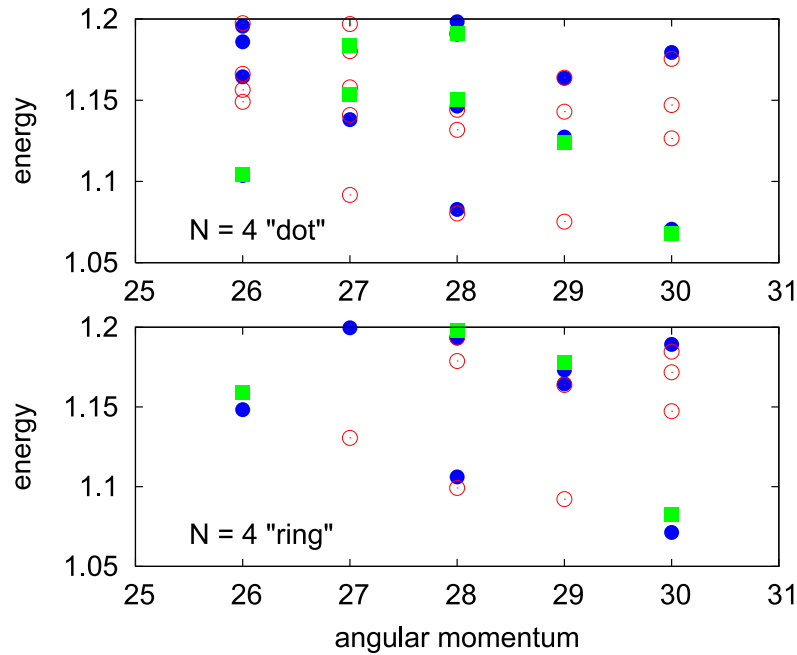
Figure 16. Energy spectrum for four electrons in a quantum dot ($\ell_{min} = 0$, $\ell_{max} = 11$) compared to that of a quasi-one-dimensional quantum ring ($\ell_{min} = 3$, $\ell_{max} = 11$) determined by restricting the basis as explained in the text. Blue points: $S = 2$, open circles: $S = 1$, green squares: $S = 0$.

an anti-ferromagnetic spin arrangement in agreement with the Heisenberg model [39], while for the dot the result is different. Note, however, that in both cases we observe the separation of the lowest, purely rotational band, with the same sequence of spin states at each angular momentum.

Figure 17 shows examples of the pair correlation functions, equation (3), for four electrons in the purely rotational states. We can see that for the fully polarized states, i.e. the first state for $L = 34$ and second state for $L = 38$, the up–up and up–down pair correlations are similar due to the symmetry of the ferromagnetic state (we show the $S_z = 0$ result), while for spin singlet states ($S = 0$) the pair correlations show a tendency for antiferromagnetism. It is important to note also that the two states for $L = 34$ and 38 are similar, but of opposite order in energy. However, the energy differences are extremely small, as seen in figure 16.

For polarized electrons it is possible to perform an exact diagonalization for large angular momenta where the localization of electrons is clearly seen [35]. The spin degree of freedom, however, increases the available Fock space drastically. For example, for $N = 7$ or 8 electrons we are limited to study only the region up to $\nu \approx 1/3$. However, we can see that the localization begins already in this region. Figure 18 shows the pair correlation function for seven electrons at $L = 51$ corresponding to the filling factor $\nu = 2/5$. The total correlation function, equation (4), shown in the upper row of figure 18, shows clearly that the electrons begin to localize in a geometry where one electron is at the centre, and the remaining six electrons form a hexagon around it. The lowest energy state at this angular momentum is well separated from the excited states and can be approximately described by the Halperin–Haldane wavefunction, as mentioned above. It is interesting to note that in this state the electrons are not as well localized as in the excited states (fourth, fifth and seventh state). The eighth state is above
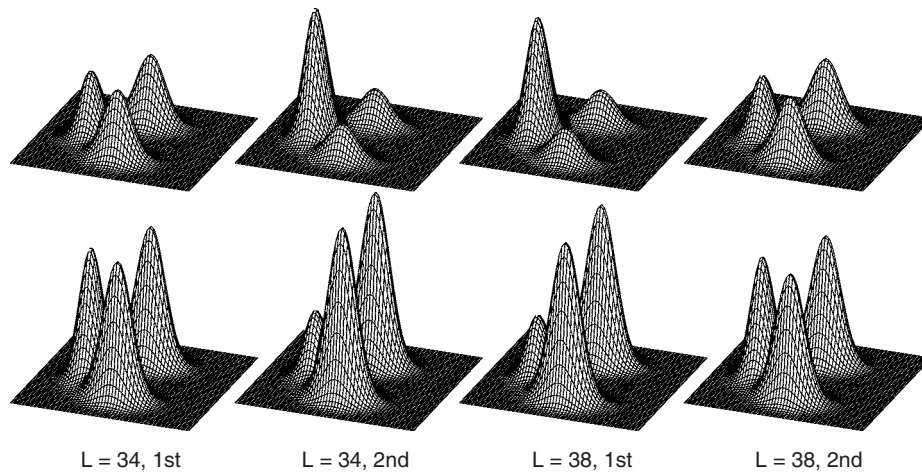
Figure 17. Pair correlation functions for $N = 4$ at angular momenta $L = 34$ and 38 for the two lowest energy states. The upper row shows the up–up correlation, $g_{\uparrow,\uparrow}$, and the lower row the up–down correlation, $g_{\uparrow,\downarrow}$. The position of the reference electron is shown as a cross ($\ell_{max} = 29$).
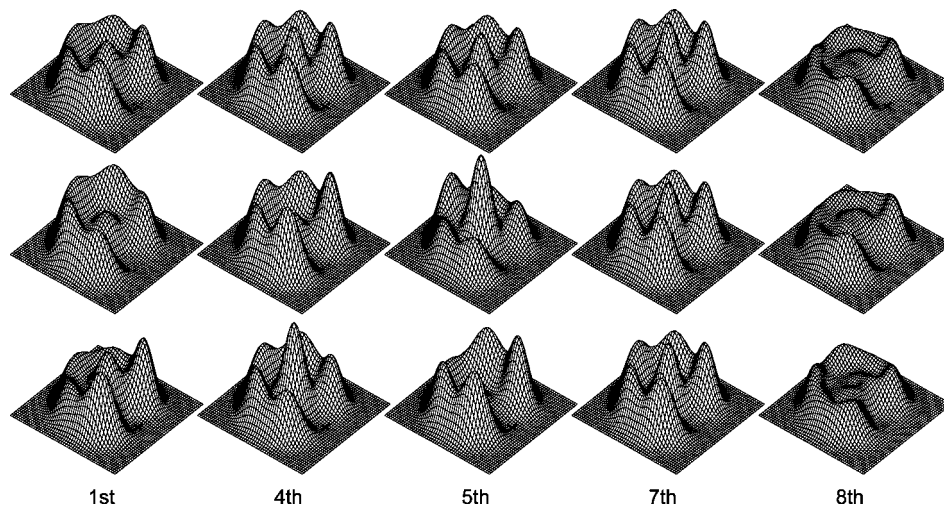

Figure 18. Pair correlation functions for $N = 7$ at angular momenta $L = 51$ for the lowest energy state (first), and for selected higher energy states (fourth, fifth, seventh and eighth). The uppermost row shows the total correlation function, $(g_{\uparrow,\uparrow} + g_{\uparrow,\downarrow})/2$, the centre row the up–up correlation $g_{\uparrow,\uparrow}$, and the lowest row the up–down correlation, $g_{\uparrow,\downarrow}$. The position of the reference electron is shown as a cross ($\ell_{max} = 19$).

the large energy gap seen in figures 11 and 13. In this state, the electrons are not as clearly localized as in the lower-lying states. This is in agreement with the start of the separation of the spin excitations from the charge excitations. Below the large energy gap in figure 13 all the excitations are spin excitations, which do not markedly change the pair correlation function, while above the gap, the excitations include a charge excitation which necessarily changes the pair correlation. We checked the pair correlations for all the states from $L = 51$ to 75. In all

cases, the states below the energy gap are similar, showing the localization of electrons which gradually becomes stronger when the angular momentum increases [35].

Figure 18 also shows the up–up and up–down pair correlations. These support the view that the low-energy excitations are mainly spin excitations. The three $S = 1/2$ states below the energy gap (i.e. the first, fourth and fifth state) show different up–up and up–down correlations, while the total correlation is nearly similar. In the case of the lowest energy state, the up–up and up–down correlations are in agreement with the Halperin–Haldane state. The repulsion between opposite spins is larger than that between the same spins.

The pair correlation functions shown in figure 18 do not show much similarity to those we obtained in the anti-ferromagnetic Heisenberg model.

Note that, in the fully polarized case, $S = 7/2$, the up–up and up–down correlations, calculated for $S_z = 1/2$, are identical, as expected.

4. Conclusions

We have studied rotational states of interacting electrons in a two-dimensional quantum dot confined by a circular harmonic potential. The many-particle Hamiltonian was solved by numerical diagonalization in a basis restricted to the lowest Landau level. The results were analysed in terms of the total angular momentum and spin. Magnetic fields were not considered explicitly, and consequently no Zeeman splitting was introduced.

The smallest possible angular momentum in the LLL is a 'double maximum density droplet' with $L = N(N-2)/4$ corresponding to the filling factor $\nu = 2$. Increasing the angular momentum the total spin of the system increases oscillating between zero and the next maximum until it reaches the fully polarized ferromagnetic state of the maximum density droplet. This behaviour was found to be the same for the long-range Coulomb interaction and for a contact interaction.

Beyond the MDD, the lowest energy states are spin waves of the ferromagnetic state in agreement with previous calculations with different periodic boundary conditions. Increasing the angular momentum further, the lowest energy states seem to consist of ferromagnetic domains, while the total spin of the system is zero.

For low total spin we did not find any vortices as low-energy excitations, although for the polarized case they appear as the lowest energy states at certain angular momenta.

The excitation spectrum shows a clear reflection symmetry around angular momentum $L = N(N-1)$ corresponding to a filling factor $\nu = 1/2$. In the neighbourhood of angular momenta $L = N(N-1)/2 + N^2/4$ and $L = 3N(N-1)/2 - N^2/4$, corresponding to filling factors 2/3 and 2/5 respectively, the spectra look very similar. Both states have $S = 0$ and a large energy gap to the first excited state. In fact, these energy gaps are the largest in the whole region from $\nu = 1$ to 1/3, apart from those in the immediate vicinity of filling factor $\nu = 1$. The lowest energy state with filling factor $\nu = 2/5$ can be rather accurately approximated by the Halperin–Haldane generalization of the Laughlin wavefunction, at least for small numbers of electrons.

In addition, the spectra are symmetric around angular momenta $L = N(N-1)/2$ and $L = 3N(N-1)2$, corresponding to filling factors 1 and 1/3, respectively. In particular, the states around $\nu = 1/3$ seem to have similar spin wave excitations to the states around filling factor one. Very recently, Dethlefsen *et al* [69] have studied the details of the excitation in the region of $\nu \approx 1/3$ with comparison to experiments.

At large angular momenta, the electrons start to localize. In the case of four electrons, accurate results could be obtained up to angular momenta $L \leqslant 46$, corresponding to a filling factor smaller than $\nu = 1/7$. In this case the results showed a clear separation of

charge-like and spin-like excitations. The charge excitations could be quantitatively explained by quantization of the classical vibrational modes of the localized electrons. However, contrary what we expected (for localized electrons) the spin excitations could not be explained within a simple Heisenberg model.

Acknowledgments

References

[1] Chakraborty T 1999 *Quantum Dots: A Survey of the Properties of Artificial Atoms* (Amsterdam: North-Holland)
[2] Reimann S M and Manninen M 2002 *Rev. Mod. Phys.* **74** 1283
[3] Chamon C and Wen X G 1994 *Phys. Rev.* B **49** 8227
[4] Reimann S M, Koskinen M, Manninen M and Mottelson B 1999 *Phys. Rev. Lett.* **83** 3270
[5] Brey L and Tejedor C 2002 *Phys. Rev.* B **66** 041308
[6] Wójs A, Gładysiewics A, Wodziński D and Quinn J J 2005 *Can. J. Phys.* **99** 1
[7] Vyborny K 2006 *Preprint* cond-mat/0603455
[8] Saarikoski H, Harju A, Puska M J and Nieminen R M 2004 *Phys. Rev. Lett.* **93** 116802
[9] Toreblad M, Borgh M, Koskinen M, Manninen M and Reimann S M 2004 *Phys. Rev. Lett.* **93** 090407
[10] Toreblad M, Yu Y, Reimann S M, Koskinen M and Manninen M 2006 *J. Phys. B: At. Mol. Opt. Phys.* **39** 2721
[11] Tavernier M B, Anisimovas E and Peeters F 2004 *Phys. Rev.* B **70** 155321
[12] Saarikoski H, Reimann S M, Räsänen E, Harju A and Puska M J 2005 *Phys. Rev.* B **71** 035421
[13] Hawrylak P, Wojs A and Brum J A 1996 *Phys. Rev.* B **54** 11397
[14] Hawrylak P, Gould C, Sachrajda A, Feng Y and Wasilewski Z 1999 *Phys. Rev.* B **59** 2801
[15] Salis G, Kato Y, Ensslin K, Driscoll D C, Gossard A C and Awschalom D D 2001 *Nature* **414** 621
[16] Eom J, Cho H, Kang W, Campman K L, Gossard A C, Bichler M and Wegscheider W 2000 *Science* **289** 2320
[17] Morf R and Halperin B I 1986 *Phys. Rev.* B **33** 2221
[18] Wu X G and Jain J K 1994 *Phys. Rev.* B **49** 7515
[19] Oaknin J H, Martín-Moreno L and Tejedor C 1996 *Phys. Rev.* B **54** 16850
[20] Karlhede A and Lejnell K 1997 *Physica* E **1** 42
[21] Fal'ko V I and Iordanskii S V 1999 *Phys. Rev. Lett.* **82** 402
[22] Lejnell K, Karlhede A and Sondhi S L 1999 *Phys. Rev.* B **59** 10183
[23] Walliser H 2001 *Phys. Rev.* B **63** 075310
[24] Smet J H, Deutschmann R A, Wegscheider W, Abstreiter G and von Klitzing K 2001 *Phys. Rev. Lett.* **86** 2412
[25] Wójs A and Quinn J J 2002 *Phys. Rev.* B **66** 045323
[26] Milovanović M V 2003 *Phys. Rev.* B **67** 205321
[27] Doretto R L, Caldeira A O and Girvin S M 2005 *Phys. Rev.* B **71** 045339
[28] Laughlin R B 1983 *Phys. Rev.* B **27** 3383
[29] Manninen M, Viefers S, Koskinen M and Reimann S M 2001 *Phys. Rev.* B **64** 245322
[30] Stone M, Wyld H W and Schult R L 1991 *Phys. Rev.* B **41** 14156
[31] http://www.caam.rice.edu/software/ARPACK
[32] Maksym P A 1996 *Phys. Rev.* B **53** 10871
[33] MacDonald A H, Yang S R E and Johnson M D 1993 *Aust. J. Phys.* **46** 345
[34] Maksym P A, Imamura H, Mallon G P and Aoki A 2000 *J. Phys.: Condens. Matter* **12** R299
[35] Reimann S M, Koskinen M, Yu Y and Manninen M 2006 *New J. Phys.* **8** 59
[36] Nikkarila J-P and Manninen M 2007 *Solid State Commun.* **141** 209
[37] Kolomeisky E B and Straley J P 1996 *Rev. Mod. Phys.* **68** 175
[38] Koskinen M, Manninen M, Mottelson B and Reimann S M 2001 *Phys. Rev.* B **63** 205323
[39] Viefers S, Koskinen P, Singha Deo P and Manninen M 2004 *Physica* E **21** 1
[40] Wensauer A, Korkusinski M and Hawrylak P 2003 *Phys. Rev.* B **67** 035325
[41] Ho T L 1994 *Phys. Rev. Lett.* **73** 874
[42] Fertig H A, Brey L, Cote R and MacDonald A H 1994 *Phys. Rev.* B **50** 11018

[43] Ruuska V and Manninen M 2005 *Phys. Rev.* B **72** 153309
[44] Ashcroft N W and Mermin N D 1976 *Solid State Physics* (Philadelphia, CA: Saunders College)
[45] Heinonen O, Kinaret J M and Johnson M D 1999 *Phys. Rev.* B **59** 8073
[46] Freeman A J, Nakamura K and Ito T 2004 *J. Magn. Magn. Mater.* **272** 1122
[47] Abolfath M, Radzihovsky L and MacDonald A H 2002 *Phys. Rev.* B **65** 233306
[48] Chalker J T, Polyakiv D G, Evers F, Mirlin A D and Wölfle P 2002 *Phys. Rev.* B **66** 161317
[49] Rezayi E H, Jungwirth T, MacDonald A H and Haldane F D M 2003 *Phys. Rev.* B **67** 201305
[50] Yang S-R E, MacDonald A H and Johnson M D 1993 *Phys. Rev. Lett.* **71** 3194
[51] Manninen M, Reimann S M, Yu Y and Toreblad M 2005 *Phys. Rev. Lett.* **94** 106405
[52] Reimann S M, Koskinen M, Yu Y and Manninen M 2006 *Phys. Rev.* A **74** 043603
[53] Jain J K 1989 *Phys. Rev.* B **40** 8079
[54] Jain J K and Kamilla R K 1998 *Composite Fermions: A Unified View of the Quantum Hall Effect*
        ed O Heinonen (River Edge, NJ: World Scientific)
[55] Kamilla R K and Jain J K 1995 *Phys. Rev.* B **52** 2798
[56] Halperin B I 1984 *Phys. Rev. Lett.* **52** 1583
[57] Balatsky A and Fradkin E 1991 *Phys. Rev.* B **43** 10622
[58] Yannouleas C and Landman U 2002 *Phys. Rev.* B **66** 115315
[59] Girvin S M and Jach T 1983 *Phys. Rev.* B **28** 4506
[60] Wójs A and Hawrylak P 1997 *Phys. Rev.* B **56** 13227
[61] Lam P K and Girvin S M 1984 *Phys. Rev.* B **30** 473
[62] Bolton F and Rößler U 1993 *Superlatt. Microstruct.* **13** 139
[63] Bedanov V M and Peeters F M 1994 *Phys. Rev.* B **49** 2667
[64] Johnson B L and Kirczenow G 1993 *Phys. Rev.* B **47** 10563
[65] Tinkham M 1964 *Group Theory and Quantum Mechanics* (New York: McGraw-Hill)
[66] Koskinen P, Koskinen M and Manninen M 2002 *Eur. Phys. J.* B **28** 483
[67] Vollhardt D 1994 *Proc. Int. School of Physics 'Enrico Fermi' Course CXXI* (Amsterdam: North-Holland)
[68] Jefferson J H and Häusler W 1996 *Phys. Rev.* B **54** 4936
[69] Dethlefsen A F, Haug R J, Výborný K, Čertík O and Wójs A 2006 *Preprint* cond-mat/0603455